

RESEARCH

Open Access



Impact of volcanic ash from Cotopaxi-2015 and Tungurahua-2016 eruptions on the dielectric characteristics of suspension insulators, Ecuador

Juan Ramírez¹, Francisco J. Vasconez^{2*}, Alex López³, Fausto Valencia¹, Franklin Quilumba¹, Anais Vásconez Müller⁴, Silvana Hidalgo² and Benjamin Bernard²

Abstract

In Ecuador, a country with several active volcanoes and with four eruptions in the last decade in the continental arc, it is very likely that high-voltage transmission lines cross volcanic hazard zones on their routes. Here, we quantify the impact of fresh volcanic ash from the hydromagmatic Cotopaxi-2015 and the magmatic Tungurahua-2016 eruptions on the dielectric characteristics of ANSI 52–3 suspension insulators made of porcelain and glass, under moist conditions. The experiments include two methodologies to measure the performance of the insulators in real-time: the minimum insulator flashover voltage (FOV_{min}) and the dielectric loss factor angle. Both allow quantifying i) the critical voltage that the insulators can withstand prior to flashover occurrence and, ii) the strong fluctuating behavior that the insulators undergo in an ashy environment. Based on six contamination scenarios, we found that there is a higher chance of flashover if the insulators are completely blanketed (top and bottom) even with a fine ash layer (1 mm), than if they are covered just at the top. Our results further show that the ash of Cotopaxi-2015 eruption has a higher chance of leading to insulator failure because of its higher conductivity (i.e. higher leachate content) than that of Tungurahua-2016. Additionally, we identify two critical voltages prior to electrical flashover on the insulators of 28.25 kV and 17.01 kV for the 230 kV and 138 kV Ecuadorian transmission lines, respectively. Finally, we present a simple impact evaluation for the main Ecuadorian transmission lines based on the outcomes of this research and the official volcanic hazard maps for Cotopaxi and Tungurahua volcanoes.

Keywords: Flashover, Volcanic ash, Leachates, Insulators, Cotopaxi, Tungurahua

Introduction

High-voltage electric transmission lines cross long distances from power generation plants to reach final users in cities. On their routes these transmission lines sometimes cross volcanic hazard zones, as is the case in Ecuador, a country with three ongoing eruptions (IGEPN 2022, 2021, 2020) in addition to 33 active

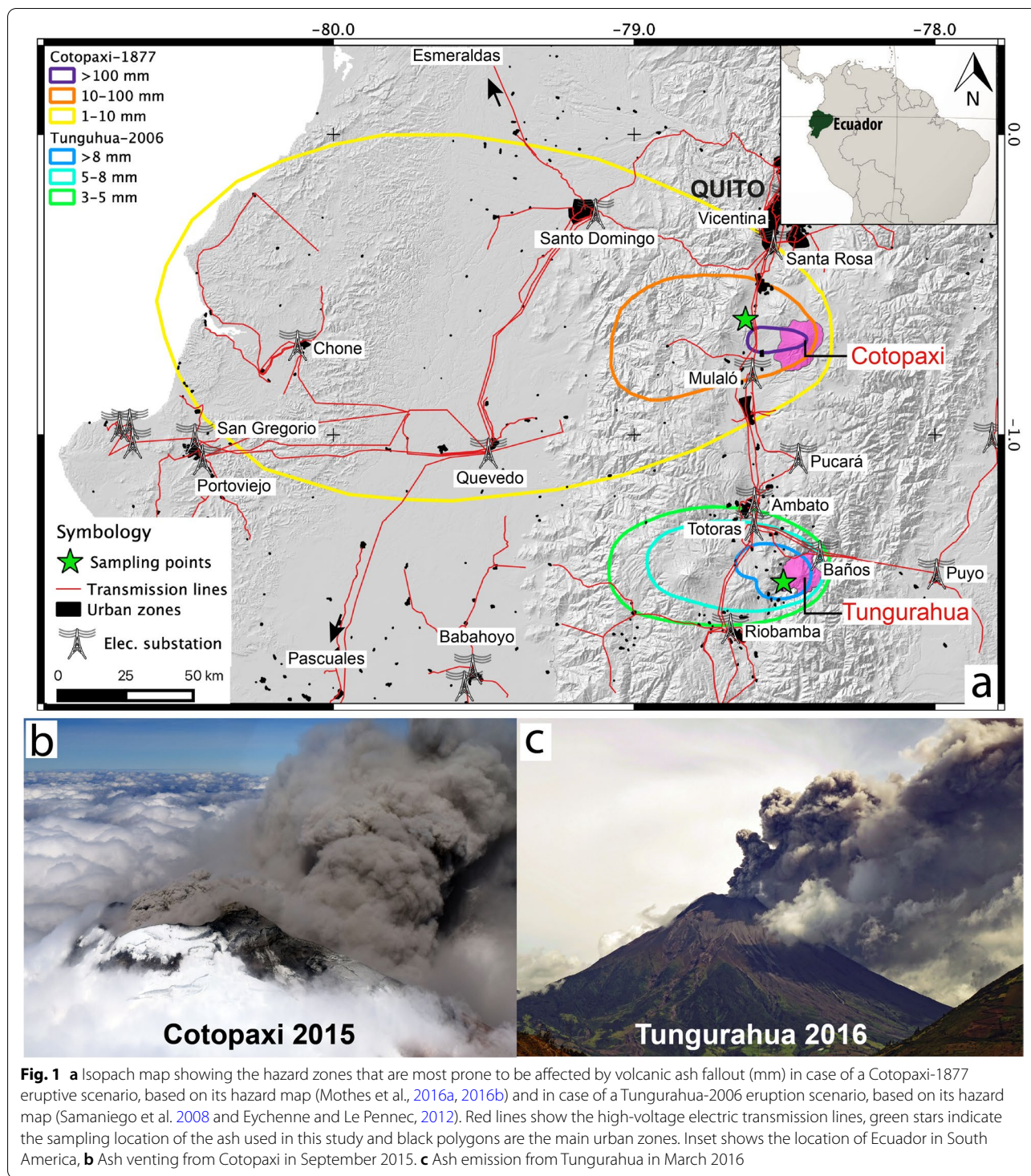
volcanoes (Ramon et al. 2021). Several main electric transmission lines of the country traverse the most probable ash fallout hazard zones of Cotopaxi and Tungurahua volcanoes, respectively (Fig. 1). These are two highly studied volcanoes that have both been active in the last two decades (Bernard et al. 2016a; Le Pennec et al. 2012; Mothes et al. 2015). Previous research has shown that ash pollution can have a negative impact on the electrical insulation quality of high-voltage electric transmission lines (Wardman et al. 2014; Wardman et al. 2012; Wilson et al. 2012). Therefore, eruptive

*Correspondence: fjasconez@igepn.edu.ec

² Instituto Geofísico, Escuela Politécnica Nacional, Quito, Ecuador
Full list of author information is available at the end of the article



© The Author(s) 2022. **Open Access** This article is licensed under a Creative Commons Attribution 4.0 International License, which permits use, sharing, adaptation, distribution and reproduction in any medium or format, as long as you give appropriate credit to the original author(s) and the source, provide a link to the Creative Commons licence, and indicate if changes were made. The images or other third party material in this article are included in the article's Creative Commons licence, unless indicated otherwise in a credit line to the material. If material is not included in the article's Creative Commons licence and your intended use is not permitted by statutory regulation or exceeds the permitted use, you will need to obtain permission directly from the copyright holder. To view a copy of this licence, visit <http://creativecommons.org/licenses/by/4.0/>. The Creative Commons Public Domain Dedication waiver (<http://creativecommons.org/publicdomain/zero/1.0/>) applies to the data made available in this article, unless otherwise stated in a credit line to the data.



activity in Ecuador could hinder the continuity of the power supply and produce blackouts in several cities of the country, including Quito (Fig. 1a), the capital city with more than 2.7 million inhabitants (INEC 2020).

Insulators are structural elements of electric transmission lines that are used to connect conductors to poles or transmission towers (Fig. 2a). Because power transmission occurs at high voltages (i.e. >1 kV), insulators are required to be made of a low conductive material to

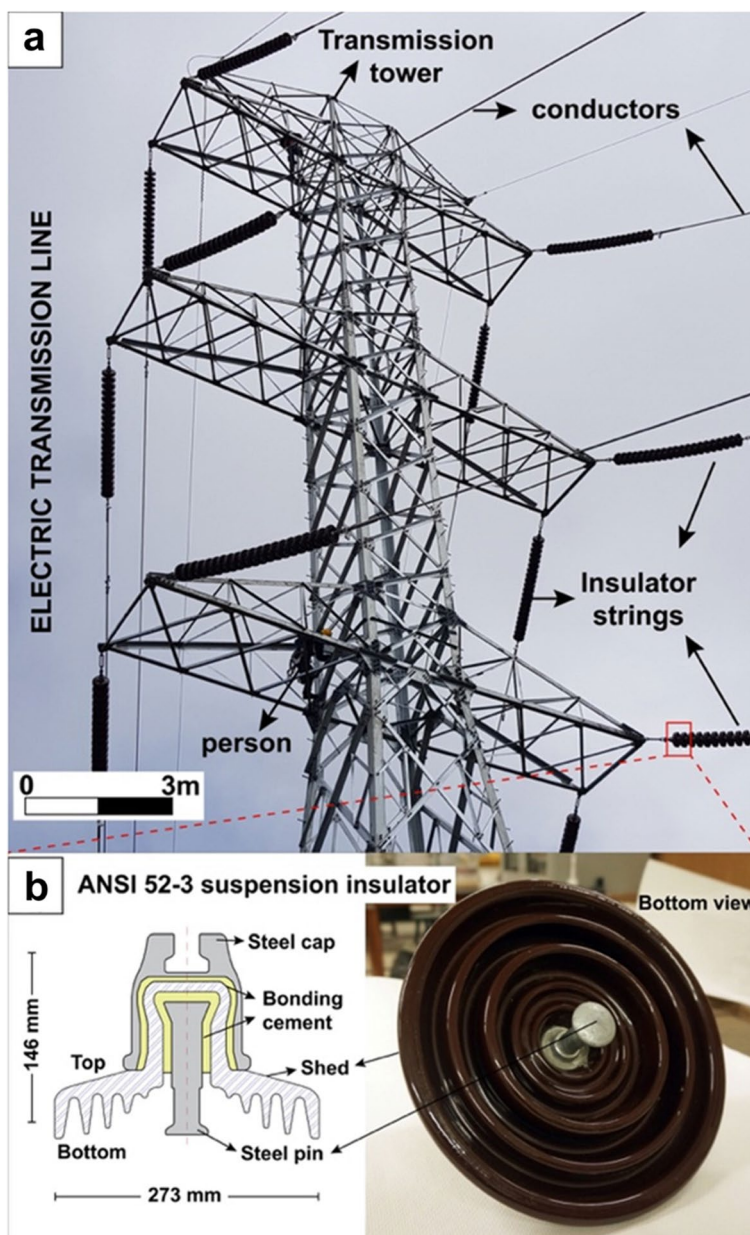


Fig. 2 **a** Overhead electric transmission line as seen from the ground. Its main structural parts are conductors, insulator strings and the transmission tower. Note the person for scale. **b** ANSI 52–3 string unit insulator schema with its main parts and bottom view picture of a porcelain insulator. This insulator is one of the most used ones in Ecuadorian electric transmission lines

clasp the conductors to the supporting structure without allowing an electric current flow (Kuffel et al. 2000). According to IEC (1993), insulators are divided into four types based on their application: pin insulators, line post insulators, string unit insulators and insulators for overhead electric traction lines. In our study, we focused on ANSI C52-3 string unit insulators because they are the ones used in most Ecuadorian electric transmission

lines. These types of insulators are made of glass or porcelain (Fig. 2b) and they are assembled forming a string of insulators of adequate length to withstand the required electrical voltage in the transmission line (IEC 1993). For Ecuador the string has between 14 to 20 insulators for a transmission line of 230 kV and between 10 and 14 insulators for a transmission line of 138 kV. However, these numbers can vary based on the altitude at which the line

is located. The distribution of the equipotential lines in a string of insulators depends on various factors, such as: the shape of the structure that supports them, the distance from the structure to the string, the number of insulators, and the effect of the corona ring parameters on the insulator (Ashouri et al. 2010). These strings can be aligned vertically and/or horizontally depending on the conductors' mechanical layout (Fig. 2a). As a rule, an electrical insulation failure is considered when an insulator allows the flow of an electric current between the conductors and the poles or transmission towers (Kuffel et al. 2000). Depending on the severity of the failure, the insulators can fracture to different degrees up to total breakage and drop the conductors to the ground. Moreover, conduction of currents through the insulator's surface in the form of electric arcs (flashover) can ignite fires and destroy the surrounding equipment. Finally, the current flow through the supporting structures, considered a short circuit, produces blackouts and cuts in the power supply.

According to Wardman et al. (2012), fresh volcanic ash is a natural pollutant composed of non-soluble and soluble particles. Volcanic ash is not an electrical conductor when dry, but under moist conditions conductive compounds (ions) leach from the ash. Some of these leachates can originate from the ash itself (e.g. from hydrothermally altered grains), as is the case of magnesium (Mg^{2+}), sodium (Na^+), calcium (Ca^{2+}) and potassium (K^+), whilst others (e.g. Cl^- , F^- , SO_4^{2-}) precipitate from the volcanic gas-phase during interaction with ash particles during an eruption (Delmelle et al. 2007; Delmelle et al. 2000). Volcanic gases and tephra are expelled together from the vent into the atmosphere and travel tens to hundreds of kilometers downwind in the eruptive plume (Witham et al. 2005). The condensation of magmatic gases, such as HCl, HF and H_2SO_4 , on ash surfaces promotes an adsorption processes of volatile elements, in particular of chloride (Cl^-) and fluoride (F^-) (Delmelle et al. 2007; Taylor and Stoiber 1973). In addition, volatilization of hydrothermal systems or crater lakes may increase the leached material that ashes can adsorb, such as sulfide (S^{2-}), sulfate (SO_4^{2-}) and others because of their higher availability (Witham et al. 2005). Importantly, when these ions precipitate on insulators, they can affect their dielectric characteristics (Wardman et al. 2014; Wardman et al. 2012; Wilson et al. 2014).

Furthermore, eruption style, magnitude and magma chemistry will influence the amount and composition of the leachate (Giggenbach 1996; Witham et al. 2005). The eruptive style will control the ratio of gas and solid particles in the eruptive plume, particle size and transport time, which all determine gas-particle interactions and hence the degree of volatile adsorption by the

ash particles (Armienta et al. 2002; Delmelle et al. 2007; Delmelle et al. 2005). For instance, the finer the ash particles and the more irregular their surface, the greater their volatile adsorption capacity due to their higher surface-to-volume ratio (Armienta et al. 2002; Rubin et al. 1994). Moreover, moist atmospheric conditions promote adsorption processes and increase the adherence of the ash to the exposed electrical insulator areas (Wilson et al. 2014). Importantly, fine ash particles of recent volcanic fallout deposits can be resuspended under dry and windy conditions (Folch et al. 2014; Forte et al. 2018), and increase insulator exposure to ash contamination even after the eruption has ended.

Investigations carried out by Wilson et al. (2014) about the effect of leachable elements of pseudo-ash on electric insulators showed that, under moist conditions, residual contamination could result in: i) a decrease in the insulation quality, ii) excessive leakage current, iii) constant flaring that causes deterioration of the insulator, and iv) discharges on the insulator surface. Driven by those observations, the purpose of the present manuscript is to take advantage of the two most recent and well-studied eruptions of Cotopaxi and Tungurahua volcanoes and to go beyond the volcanological analysis to quantify the effects of two different types of fresh volcanic ash (hydro-magmatic and magmatic, respectively) on electrical insulation properties under moist conditions. The effects were measured in real-time on the dielectric quality of the ANSI 52–3 suspension insulators made of porcelain and glass, which are the most commonly installed ones on the 230 kV and 138 kV transmission lines in Ecuador.

Cotopaxi and Tungurahua recent eruptive history

This section presents the broad context of the eruptive histories of Cotopaxi and Tungurahua volcanoes and a detailed description of their most recent eruptive periods, which took place in 2015 and from 1999 to 2016, respectively. This information is based on several published papers, theses and technical reports provided by the Instituto Geofísico of the Escuela Politécnica Nacional (IG-EPN), which is the official entity in charge of monitoring volcanic and seismic activity in Ecuador.

Cotopaxi (78.43°W, 0.68°S, 5897 m asl) is an active volcano, located 50 km south of Quito (Fig. 1a). It has an extensive glacier cap that covers ~ 11 km² (Cáceres 2016). During historical times, it had five main eruptive cycles and at least 13 paroxysmal eruptions (Barberi et al. 1995; Pistolesi et al. 2011). The eruptions triggered devastating primary lahars due to sudden glacier melting during pyroclastic flow emplacement (Mothes et al. 2004; Sierra et al. 2019). Additionally, the eruptions blanketed large areas with volcanic material, which is one of the most long-term hazards related to this volcano (Biass

and Bonadonna 2013). The most recent major eruption of Cotopaxi took place in 1877 AD (Sodiro 1877; Wolf 1878). This eruption has been considered by the IG-EPN as the most probable worst-case scenario for the elaboration of the volcanic hazard maps of Cotopaxi (Fig. 1a; Mothes et al. 2016b, 2016a). After 73 years of quiescence, from August to November 2015, Cotopaxi had a minor eruptive period (Hidalgo et al. 2018). This period was characterized by a highly explosive vent-opening phase, which expelled up to 8 km high eruptive plumes. Afterwards, the eruptive period evolved to phases of continuous ash venting (Bernard et al. 2016a, Fig. 1b). During this period, ash fallout was the main volcanic hazard, affecting cities as far as 260 km away from the vent, mainly those located towards the west of the volcano (Bernard et al. 2016a). Recent investigations have demonstrated that the rising magma of Cotopaxi 2015 came into contact with the underground hydrothermal system producing hydromagmatic explosions during its first stages (Calahorrano-Di Patre et al. 2019; Gaunt et al. 2016). Based on the data presented in Gaunt et al. (2016), hydrothermally altered material on average made up 18% of the tephra components ejected by Cotopaxi between 15 August and 23 November 2015 at 6 km from the vent (Fig. 3a), and, at the same sampling location, 44% of the fall deposits corresponded to fine ash (< 63 μm , F2, Fig. 3b).

Tungurahua (78.44°W, 1.46°S, 5016 m asl), located 140 km south of Quito (Fig. 1a), is one of the most active volcanoes in Ecuador. Its historical eruptive periods have lasted on average 12 years and have been separated by quiescence periods of about one century (Hall et al. 1999). This andesitic volcano has had notable eruptive activity since 700 yBP, producing regional ash and scoria fallout and major pyroclastic currents (Le Pennec et al. 2008). Tungurahua's last eruptive period lasted from October 1999 (Le Pennec et al. 2012) until March 2016 (IGEPN 2018). This period was characterized by various eruptive phases separated by weeks to months of quiescence (Hidalgo et al. 2015). The most common volcanic phenomenon was the emissions of ash plumes, which reached various kilometers above the crater level (Arellano et al. 2008; Eychenne and Le Pennec 2012; Hidalgo et al. 2015; Mothes et al. 2015), mainly affecting the areas located to the west of the volcano, which corresponds to the prevailing wind direction (Parra et al. 2016). In addition, occasional major eruptions generated pyroclastic currents that traveled as far as the volcanic ring plane, about 7–8 km from the crater (Bernard et al. 2016b; Gaunt et al. 2019; Hall et al. 2015). Local rainfall often remobilized the recently deposited loose material, triggering secondary lahars (Jones et al. 2015). In August 2006, a paroxysmal eruption occurred (Andújar

et al. 2017; Bernard et al. 2016b; Samaniego et al. 2011), claiming the life of six people. Currently, this eruption considered as one of three most probable worst-case scenarios in the volcanic hazard map in case of future activity (Samaniego et al. 2008). Throughout the entire period, most of the eruptions were categorized as magmatic based on their high juvenile component content (Battaglia et al. 2019; Bustillos A. et al. 2017; Eychenne and Le Pennec 2012). Tungurahua's eruptive styles varied between Strombolian and sub-Plinian and from continuous to episodic (Hidalgo et al. 2015). Its last eruptive phase occurred in February–March 2016 (Fig. 1c). Based on geophysical and geological data, Gheri (2019) suggested that this eruption began as sub-Plinian and evolved to Vulcanian. His data also revealed that juvenile material (pumice and coarsely vesicular and blocky scoria) represented the main component (77% on average, Fig. 3a) of the ash expelled between 26 February and 10 March 2016 at one sampling location at 6 km from the vent. In addition, Gheri (2019) found a high percentage (3–30%) of oxidized lithic clasts. Finally, Gheri (2019) found that the fall deposits of the final eruptive phase of Tungurahua comprised 30% of fine ash on average (< 63 μm , F2, Fig. 3b).

Summarizing, as presented in Gaunt et al. (2016) and Gheri (2019), the ash emitted by the 2015 eruption of Cotopaxi contains a larger percentage of hydrothermally altered material (18%) than that of Tungurahua in 2016 (0%). In addition, Cotopaxi's ash is finer at the same distance from the vent (6 km) and under the same prevailing wind direction as at Tungurahua (Fig. 3b). These two parameters play a key role in determining the amount of leachates in the ash that can affect the quality of electrical insulators.

Methods

This section describes our ash sampling, the analysis of leachable elements and the methodology used to test the impact of the ash from Cotopaxi-2015 and Tungurahua-2016 eruptions on the ANSI 52–3 suspension insulators in real-time under moist conditions.

Ash sampling and leachable element analysis

We sampled 15 kg of ash from each of the aforementioned eruptions from a flat and dry surface (Fig. 1a, green stars). In the case of Cotopaxi the sample was taken from a concrete soccer field in early 2016 after the eruption had ended, while Tungurahua's ash was sampled daily from a roof during the March 2016 eruptive phase. Because of the short elapsed time between the eruptions and sampling, we assumed that most of the sample contamination came from the same reworked and resuspended ash. In a next step, the samples were dried

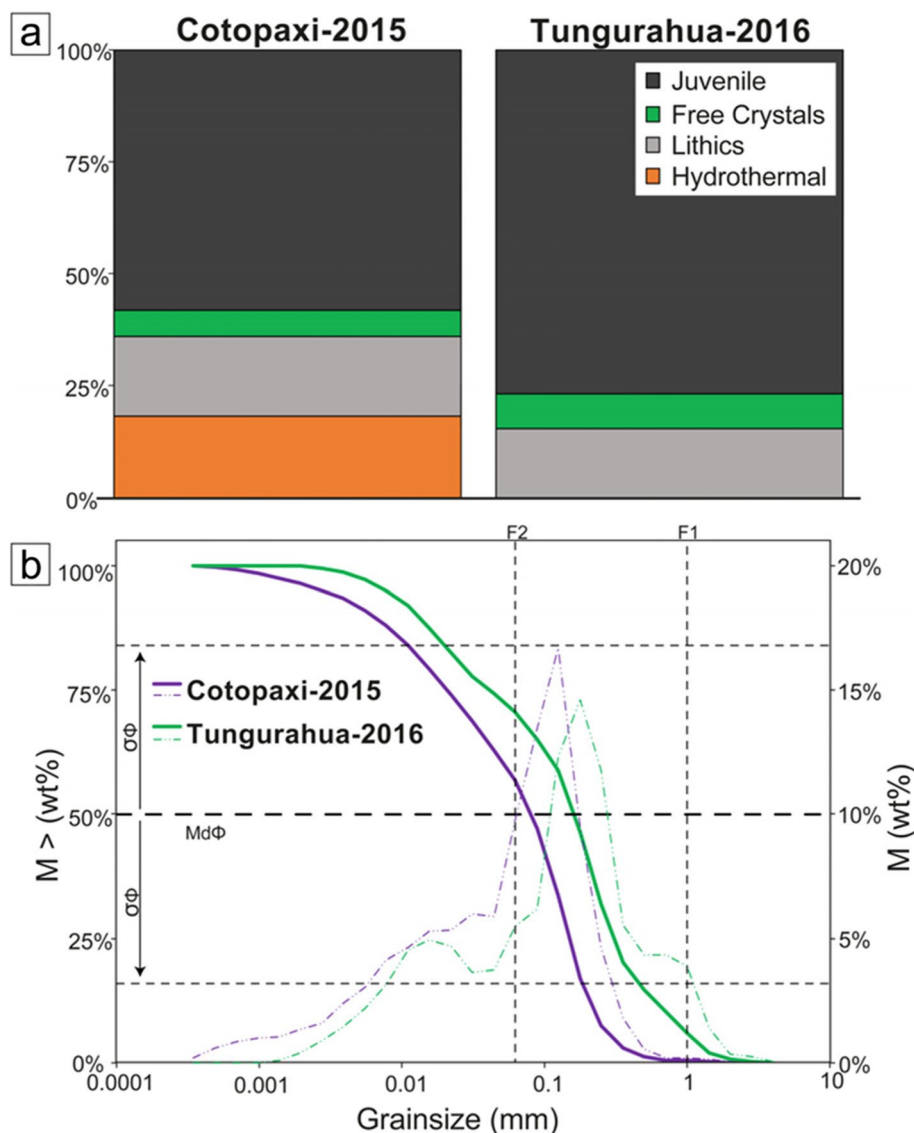


Fig. 3 **a** Component proportions for ash of Cotopaxi-2015 and Tungurahua-2016 eruptions at 6 km distance from the vent. **b** Solid lines depict the cumulative and dashed lines the weight percent grain size distributions (GSD) of Cotopaxi and Tungurahua eruptions. F1 and F2 are coarse (1 – 0.063 mm) and fine (<0.063 mm) ash thresholds, respectively. Md is the median and the sorting at D16 and D84. The graphs are based on data from Gaunt et al. (2016) and Gheri (2019)

at room temperature (20 °C) for 48 h. We used 5 g, 25 g and 50 g of the dry ash to dilute in 500 ml of deionized water to identify the main leachable elements contained within and adsorbed onto the ash particles based on the protocol proposed by Stewart et al. (2013). All possible chemical proportions were quantified at the CICAM laboratory from the Escuela Politécnica Nacional (EPN) following the standard method for the examination of water and wastewater described in APHA (2017). The chemical proportions of calcium, chloride and magnesium were calculated by using titration based on the 3500-Ca

B, 4500-Cl B and 3500-Mg B standard methods, respectively. For potassium and sulfate, we applied spectrophotometry by using the 3500-K and 4500-SO₄²⁻ E methods (APHA 2017).

Experimental set-up

The impact of volcanic ash on the dielectric properties of ANSI 52–3 suspension insulators made of glass and porcelain was measured inside an artificial pollution chamber. The chamber is a cube of 2.4 m side length installed in the High Voltage laboratory at the EPN. Insulator

quality was tested under ash pollution and moist conditions created by an air compressor that sprayed 3 mm/h of water according to the requirements of IEC (2013). The experimental procedure to measure the quality of the electrical insulation in real-time involved two methods widely applied in the industry: i) a testing procedure to identify the Minimum Insulator Flashover Voltage (FOVmin) based on ANSI/NEMA (2018) following the specifications of IEC (2013), and ii) a system to monitor the conditions of the insulator (dielectric loss factor angle).

The testing system was powered with a high voltage transformer of 100 kV/220 V, 5 kVA and 60 Hz, which is appropriate for testing the insulator given that the ANSI

52–3 can withstand 95 kV under normal conditions (i.e. no particle contamination or moisture, 1 atm and 20 °C) (ANSI/NEMA 2018). A kilovoltmeter (KVM) and a capacitive divider HIPOTRONICS represented by C1 and C2 in Fig. 4 were also used to measure the voltage applied to the insulator both with the KVM instrument and with the computer by means of an Analogue Digital Converter (ADC) and LabVIEW.

Minimum insulator flashover Voltage (FOVmin)

During each test, the failure voltage of the insulator continuously decreases as the leachates in the pollutant are dissolved due to the moisture. These leachates make the insulator become more and more conductive until a

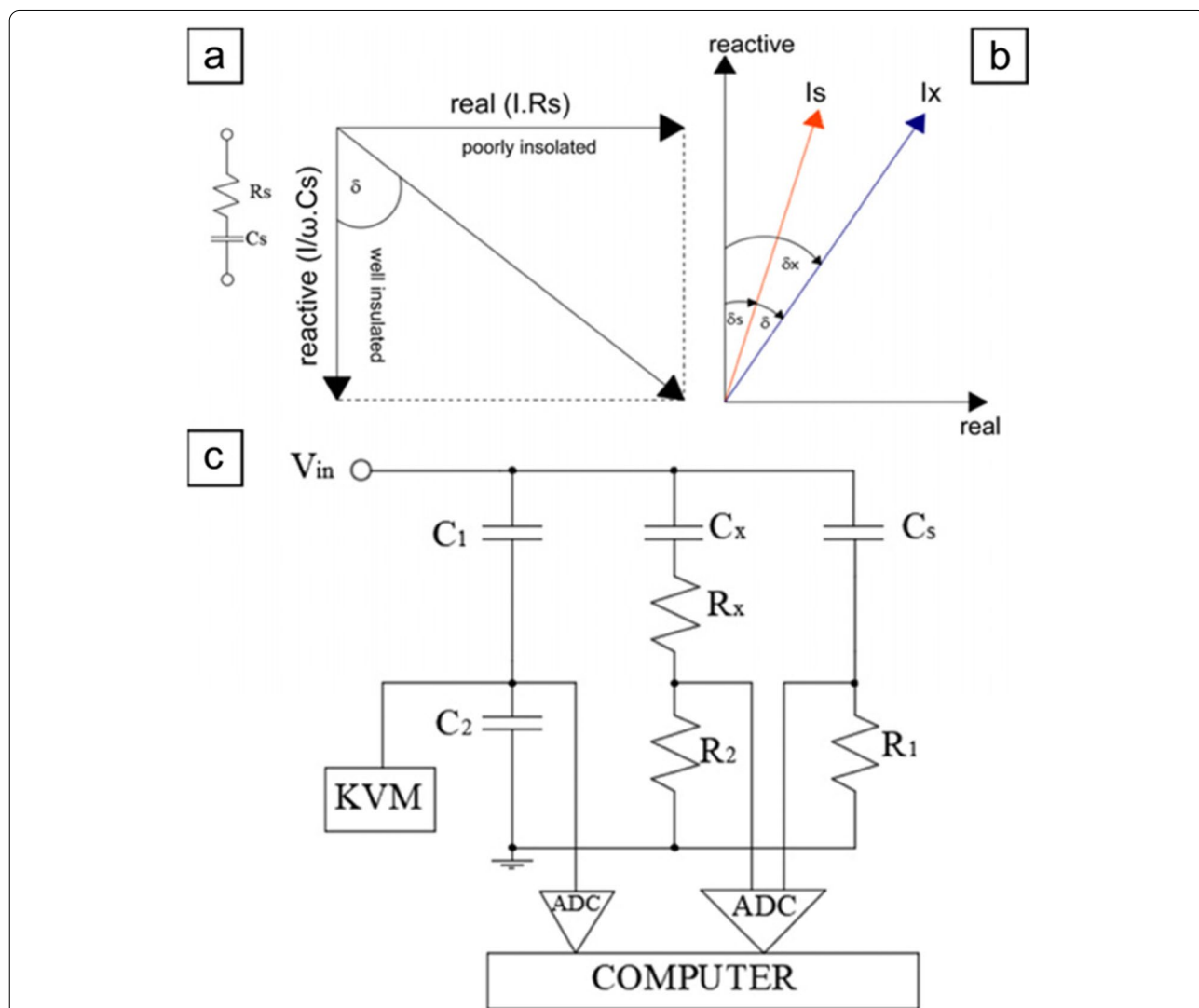


Fig. 4 a Phasor diagram of a dielectric material. Ir is the current due to losses on the insulator and Ic represents the capacitive current. b Phasor diagram of the current components of both branches. c Circuit implemented for current measurement. Rx and Cx are unknown parameters, while Cs = 99.7 pF, R1 = 265.25 Ω and R2 = 25 Ω

flashover occurs (Lambeth 1988). Therefore, the FOV_{min} is defined as the minimum voltage needed to disrupt an insulator and cause failure due to leachates that dissolve under moist conditions (IEC 2013; Lambeth 1988). Once the maximum leachate dissolution is reached, they begin to drip and wash off the insulator and it is left with a lower amount of conductive salts. Consequently, the voltage starts to increase again, forming a U-shaped curve, which allows for the minimum insulator flashover voltage to be obtained (IEC 2013). Therefore, this method allows obtaining the minimum value of power frequency voltage that would produce a discharge in an insulator contaminated with a layer of pollutant that has leachates in a humid environment.

Dielectric loss factor angle

The angle δ between the real (I.Rs) and the reactive (I/ ω . Cs) component of an electric current is the dielectric loss factor angle (Fig. 4a), which forms when alternating current (AC) voltages flow through an insulator (Kuffel et al. 2000; Wadhwa 2007). Generally, when the dielectric loss factor angle is small i.e. close to the reactive component, there is a much better insulation quality than when it is near to the real component (Fig. 4a). In this study, we quantify the dielectric loss factor angle by subtracting the angle of the current passing through the insulator (Ix) and a reference current (Is) (Kornhuber et al. 2009), as shown in Fig. 4b. The reference current (Is) is obtained by a standard capacitor for which dielectric loss is negligible (~ 0 A). Therefore, the dielectric loss angle (δ) is measured directly from Ix. The diagram of the circuit used to measure these angles is depicted in Fig. 4c, where the tested insulator is represented by a resistor (Rx) and a capacitor (Cx) mounted in series (Wadhwa 2007). The capacitance (Cs) represents the standard capacitor used as reference, while R1 and R2 are two power resistors from which voltage signals are measured. These signals enter the data acquisition card DAQ NI USB-6008 of National Instruments as analog signals and are then converted to digital using the DAQ Assistant application and the LabVIEW Electrical Power tool. This information allows to measure the current phasors that pass through R1 and R2 and which correspond to the insulator and the standard capacitor, respectively. The current phasor is a vector, where RMS (root mean square) is a scalar that depicts the AC voltages measured, and δ corresponds to the dielectric loss factor angle. R1 and R2 values must be smaller than the impedances of the standard capacitor (Cs) and the insulator (Rx) to avoid changes in the current (Ix). However, they should be high enough to produce a voltage in the order of millivolts to be read by the data acquisition system. Based on these two criteria, we estimated the R1 and R2 values by trial-and-error experimental

tests to complete the circuit (Fig. 4c). Finally, we measured Ix and Is, which then are converted to phasor to estimate δ and thus measure the conditions of the insulator in real-time.

Ash-contamination scenarios

Based on the findings of Wardman et al. (2014), we considered six of their nine pseudo-ash contamination scenarios, in which flashover occurs under moist conditions. In our study, each scenario was applied to the ANSI 52–3 insulators (porcelain and glass) with fresh volcanic ash from Cotopaxi-2015 and Tungurahua-2016 eruptions. The contamination scenarios varied based on ash-thickness (millimeters) on the top and/or bottom of the insulator surfaces (Table 1). In total, 15 kg of volcanic ash of each eruption were used: The first 6 kg were utilized to calibrate the experimental procedure, while the remaining 9 kg were employed for the testing itself. For instance, in the highest contamination scenario (6, Table 1), around 0.5 kg of ash were used per insulator type and repetition. Three repetitions were performed on both, glass and porcelain insulators, in order to verify reliability, adding up to 3 kg of ash. The remaining 6 kg were used in the other 5 scenarios.

Testing procedure

The impact of the volcanic ash from Cotopaxi-2015 and Tungurahua-2016 eruptions on the porcelain and glass ANSI 52–3 insulators was quantified by the two methods previously described. Both the FOV(min) and the dielectric loss factor angle were measured in real-time to evaluate the conditions of the insulators during each ash-contamination scenario in a moist environment.

Table 1 Volcanic ash contamination scenarios under moist conditions based on Wardman et al. (2014) and applied to both ANSI 52–3 insulator types (porcelain and glass) with ash from Cotopaxi-2015 and Tungurahua-2016 eruptions. Top and bottom refer to ash cover thickness on the bottom and top of the insulators

Ash-scenario	Top (mm)	Bottom (mm)
1	1	0
2	3	0
3	6	0
4	1	1
5	3	1
6	6	1

The electrical tests were carried out according to the following procedure, adapted from Wardman et al. (2014) after Lambeth (1988).

- 1) A clean insulator is blanketed with a uniform layer of ash on its bottom and/or top according to the scenario being investigated (Table 1). Contamination was performed by dusting until a uniform ash-coating was reached (Fig. 5a).
- 2) The contaminated insulator is installed for testing in the fog chamber.
- 3) The insulator is energized under dry conditions, and the voltage gradually increased, making sure that no discharges occur until the insulator acquires thermal equilibrium. As the insulator goes into equilibrium, the voltage keeps rising until it reaches about 70% of

its specified wet failure voltage, which was previously calculated for the atmospheric conditions at the laboratory, in accordance with the IEEE (2013).

- 4) Light rain of 3 mm/h is applied for five minutes until a discharge (flashover), or peak current occurs. If these conditions are not reached within that time, the voltage is increased every minute in steps of 10%, until a flashover or peak current occurs (Fig. 5b).
- 5) Once a flashover happens, the insulator is re-energized to 80% of the previous fault voltage as soon as possible (less than one minute). Then, the voltage is increased every two minutes in steps of 5% until a new failure occurs, or a peak current value appears.
- 6) The previous step is repeated until the minimum flashover voltage (FOVmin) is obtained. This value is identified because, after having reached the highest point of conductivity (i.e. lowest voltage) and dissolution of leachates from the volcanic ash, the fault voltage starts to increase again.
- 7) In addition, throughout the entire testing the dielectric loss factor angle is measured.
- 8) The insulator is removed from the fog chamber. The residual ash stuck to the insulator surfaces (Fig. 5c) is cleaned using deionized water (500 ml). Both, ash and water are then collected and labeled in a clean container to then measure their electrical conductivity by using a conductometer ORION 5Star and to finally determine their non-soluble deposit density (NSDD) and equivalent soluble deposit density (ESDD) levels based on (IEC 2008; Kuffel et al. 2000). The procedure for the extraction of the contaminant is based on IEC (2008).
- 9) This sequence is repeated three times for each scenario, insulator material and volcanic ash type.

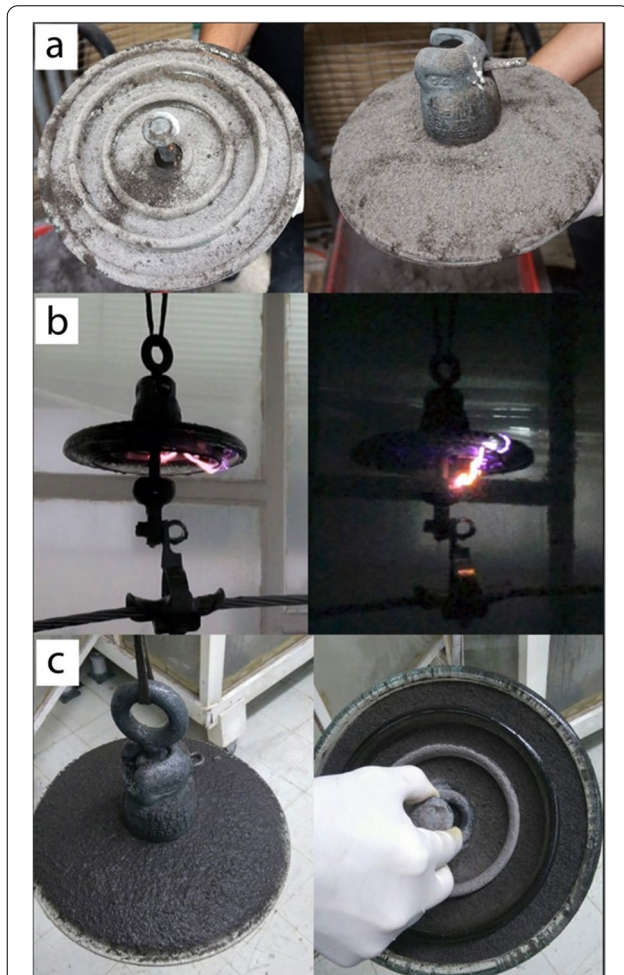


Fig. 5 **a** Fresh volcanic ash blanketing the insulator surface (bottom and top), **b** Flashover during the test under ash contamination and moist conditions in the fog chamber, **c** residual ash on the glass ANSI 52–3 insulator after testing

Degree of contamination on the insulator

Volcanic ash is considered a solid type A contaminant (Wardman et al. 2014; Wardman et al. 2012). Type A comprises an active (conductive particles) and an inert portion (non-conductive material). Therefore, the degree of contamination is determined by the ratio between the equivalent amount of material containing leachates (ESDD) and the equivalent amount of insoluble material (NSDD) in $\text{mg}\cdot\text{cm}^{-2}$ (IEC 2008). These values represent the amount of conductive and non-conductive material per square centimeter on the insulator surface. The norm to quantify the ESDD/NSDD is described in detail in IEC (2008). The degree of contamination obtained for each testing scenario is determined based on the ESDD, which depends on i) the amount of leachates in the volcanic ash and ii) the moist conditions during the ash fallout deposition, which dissolve these leachates.

Results

Main leached elements from the volcanic ash samples

The chemical analysis showed that the Cotopaxi-2015 ash leachate has significantly more calcium, potassium, and sulfate, than that of Tungurahua-2016 (Fig. 6a & 6b). In contrast, the amount of magnesium and chloride is similar in both samples over various ash/water

concentrations (Fig. 6a & 6b). Importantly, the Cl/SO₄ ratio depicted in Fig. 6c is much lower for Cotopaxi-2015 (< 1) than for Tungurahua-2016 (> 1).

Minimum insulator flashover voltage (FOVmin)

Each test lasted from 15 to 60 min depending on the ash-contamination scenario. Duration depended on the

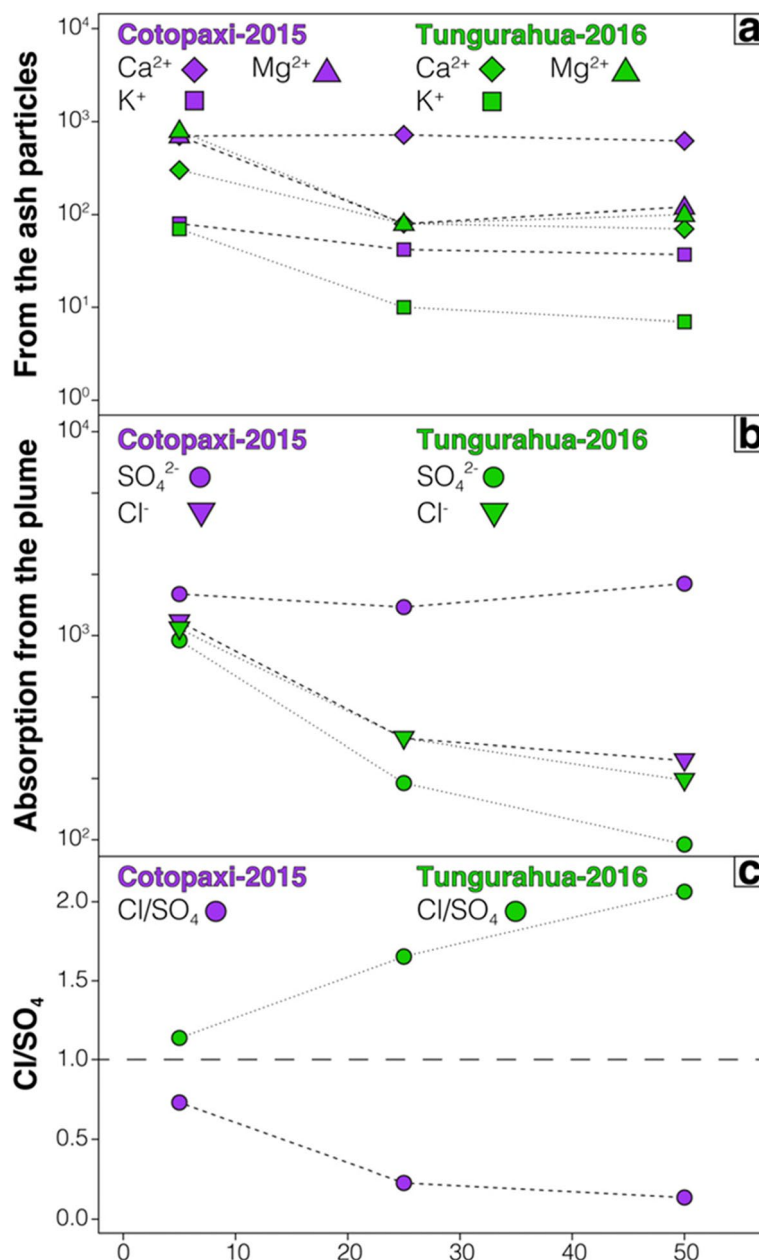


Fig. 6 Concentration (mg/kg) of various ions in volcanic ash from Cotopaxi-2015 and Tungurahua-2016 eruptions in gram per 500 ml of deionized water **a** calcium (Ca²⁺), potassium (K⁺) and magnesium (Mg²⁺) leached from the minerals inside the ash particles, **b** chloride (Cl⁻) and sulfate (SO₄²⁻) leached from adsorbed volatiles onto ash particles during gas-particle interaction and/or volatilization of a hydrothermal system, **c** Cl/SO₄ ratio. Note that figures a and b are in logarithmic scale

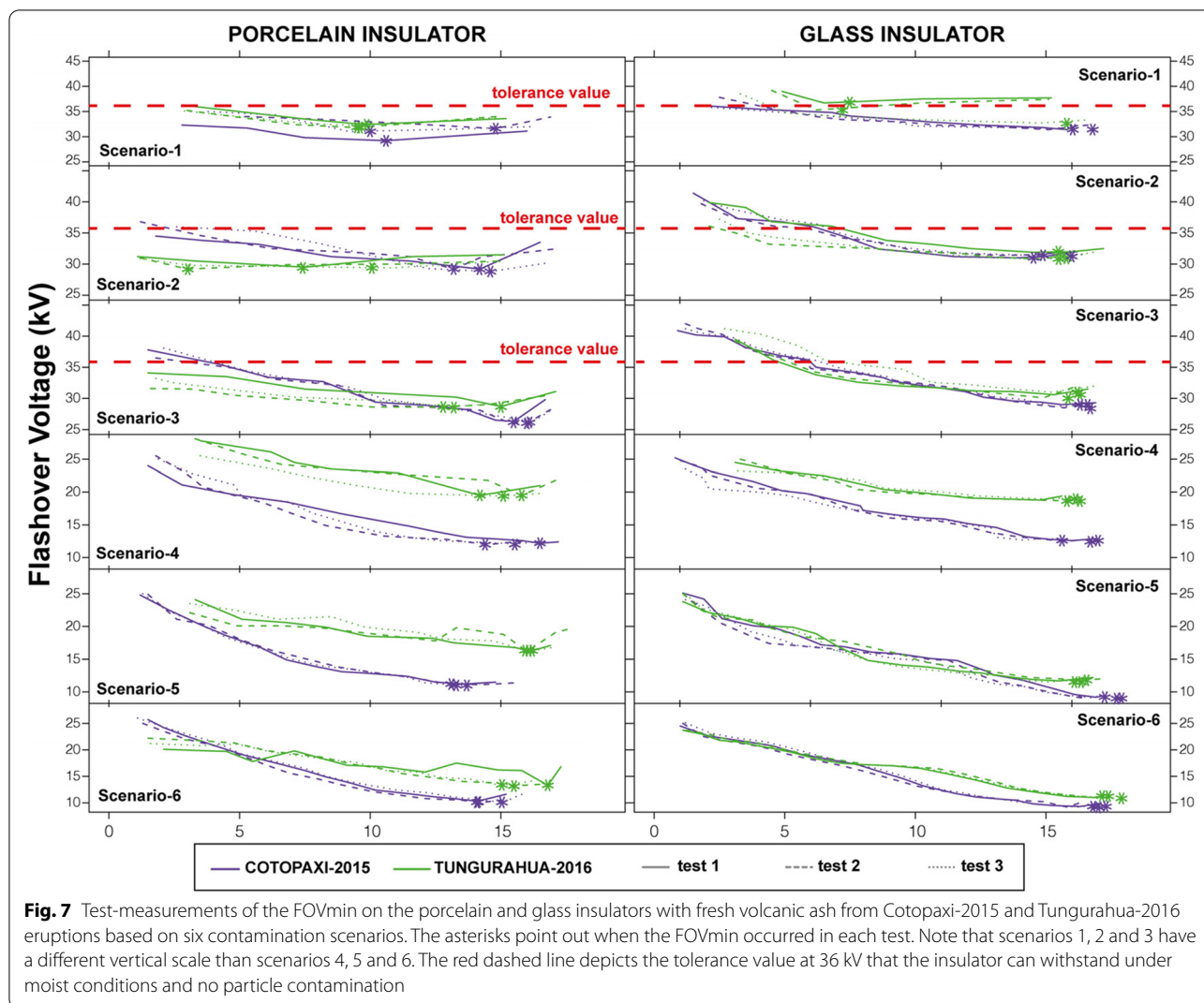


Fig. 7 Test-measurements of the FOVmin on the porcelain and glass insulators with fresh volcanic ash from Cotopaxi-2015 and Tungurahua-2016 eruptions based on six contamination scenarios. The asterisks point out when the FOVmin occurred in each test. Note that scenarios 1, 2 and 3 have a different vertical scale than scenarios 4, 5 and 6. The red dashed line depicts the tolerance value at 36 kV that the insulator can withstand under moist conditions and no particle contamination

proportion of available leachates to be dissolved (i.e. contamination scenarios in Table 1) until the FOVmin was reached. In Fig. 7 we display the last ~20 min of each analysis of the three tests performed on the porcelain and glass insulators contaminated with fresh volcanic ash from Cotopaxi-2015 and Tungurahua-2016 eruptions. Overall, the plots recorded voltage reduction over time until the minimum flashover voltage occurred (asterisks in Fig. 7), after which voltage started to increase again. FOVmin, which depended on the amount of leachates, was obtained after various repetitions. Interestingly, in scenarios 4, 5 and 6 flashover voltages were lower than in scenarios 1, 2 and 3 (note the vertical scale in Fig. 7). Additionally, in both, porcelain and glass insulators, Cotopaxi-2015 ash reached lower FOVmin voltages than that of Tungurahua-2016.

Table 2 summarizes the minimum flashover voltages for each ash-contamination scenario. In general, the

measured voltages were lower than the tolerance values specified by the insulator manufacturer for moist conditions without particle contamination. In accordance with ANSI/NEMA (2018), this specified value is 36 kV once it is corrected to the atmospheric conditions in the laboratory based on IEEE (2013).

In contamination scenarios 1, 2 and, 3 (contamination only on the top of the insulator), the lowest critical flashover voltage for the porcelain insulator was 26.0 kV for Cotopaxi-2015 and 28.6 kV for Tungurahua-2016 ash (Table 2, Fig. 7), while for the glass insulator critical voltages were 28.5 kV and 30.1 kV, respectively (Table 2, Fig. 7). Therefore, we found that the porcelain insulator is more prone to fail than the glass one in these scenarios. In contamination scenarios 4, 5 and 6 (top + bottom), the most critical flashover voltages for the porcelain insulator were 10.0 kV for Cotopaxi-2015 and 13.2 kV for Tungurahua-2016 ashes, and for the

Table 2 Minimum flashover voltages (FOVmin) according to each contamination scenario for Cotopaxi-2015 and Tungurahua-2016 ashes in kV

COTOPAXI-2015										
Scenario	Porcelain Insulator					Glass Insulator				
	Test 1	Test 2	Test 3	Average	Std	Test 1	Test 2	Test 3	Average	Std
1	29.2	31.6	31.0	30.6	1.02	31.4	31.4	31.5	31.4	0.05
2	29.2	29.2	28.8	29.1	0.19	31.0	31.5	31.3	31.3	0.21
3	26.3	26.0	26.2	26.2	0.13	29.0	28.5	28.7	28.7	0.21
4	12.2	12.0	12.1	12.1	0.08	12.6	12.5	12.9	12.7	0.17
5	11.2	11.1	11.0	11.1	0.08	9.2	9.0	9.1	9.1	0.08
6	10.3	10.0	10.1	10.1	0.13	9.3	9.2	9.2	9.2	0.05
TUNGURAHUA-2016										
Scenario	Porcelain Insulator					Glass Insulator				
	Test 1	Test 2	Test 3	Average	Std	Test 1	Test 2	Test 3	Average	Std
1	32.4	31.8	32.2	32.1	0.25	35.7	35.3	32.7	34.6	1.33
2	29.5	29.2	29.4	29.4	0.13	31.9	31.2	30.8	31.3	0.46
3	28.7	28.6	28.7	28.7	0.05	30.6	30.1	31.0	30.6	0.37
4	19.5	19.5	19.4	19.5	0.05	18.8	18.7	18.9	18.8	0.08
5	16.3	16.2	16.3	16.3	0.05	11.7	11.7	11.5	11.6	0.09
6	13.3	13.2	13.3	13.3	0.05	11.2	11.0	11.3	11.2	0.13

Note that these values are lower than 36 kV, which is the specified tolerance value for the insulators under moist conditions. Std standard deviation

glass insulator 9.0 kV and 11.0 kV, respectively (Table 2, Fig. 7). Hence, in contrast to the previous scenarios, the glass insulator is more prone to fail than the porcelain one. Additionally, the Cotopaxi-2015 ash significantly reduced the minimum flashover voltage (FOVmin) in all the investigated scenarios and in both, porcelain and glass insulators, indicating a significant negative impact on the insulation properties (Table 2, Fig. 7).

Overall, when volcanic ash was deposited also on the bottom of the insulator (scenarios 4–6), the FOVmin was significantly reduced (Fig. 7). For instance, in the case of the porcelain insulator the FOVmin is 1.7 and 2.6 times lower than in scenarios 1–3 (only top), for the ash of Tungurahua-2016 and Cotopaxi-2015, respectively. Similarly, for the glass insulator it is 1.8 and 3.4 times lower. Consequently, if volcanic ash covers the entire surface of the insulator, even with a fine layer of 1 mm, it could drastically reduce the flashover voltage to less than 20 kV (Table 2), which is ~ 16 kV lower than the specified tolerance value. Nonetheless, if the ash is deposited only on the top, which makes up 33% of the total surface of the insulator, there is a better resistance.

The standard deviation (Std) of the FOVmin for each type of insulator and scenario only in few cases exceeds 1% and the maximum is 3.85% (Table 2). These results indicate that although the flashover can be triggered by many factors, under lab conditions the error between tests is very small. Thus, the average of the FOVmin is

a good approach that could be expected under no-lab conditions.

Dielectric loss factor angle

Without particle contamination and under dry conditions, the dielectric loss factor angle δ is 13° for the porcelain insulator and 15° for the glass one. Despite the voltage variations that the insulator is withstanding, the dielectric loss factor angle remains almost constant over time. On the other hand, when the insulator is exposed to different levels of ash contamination in a moist environment, the leachates dissolve and create a conductive channel on its surface. This affects the dielectric loss factor angle (δ), which begins to increase and fluctuate strongly over time. Extreme values of approximately $\pm 180^\circ$ are observed throughout the testing and, overall, oscillations are stronger in scenarios 4 to 6 (Fig. 8). These oscillations and the increase of the loss factor angle indicate that there is an external material affecting the insulation properties. Consequently, partial discharges occur and current peaks are detected (Fig. 8). The current varies strongly at the first applications of voltage (> 1 mA) because the ions start to leach from the ash on the insulator surface (Fig. 8). Current peaks are the observable flashovers, after which the current stabilizes for various seconds at 2 mA. The maximum current peak reached 15 mA (Fig. 8). Moreover, we observed that the voltage drastically drops after a flashover occurs (Fig. 8). Even though Fig. 8 allows understanding how

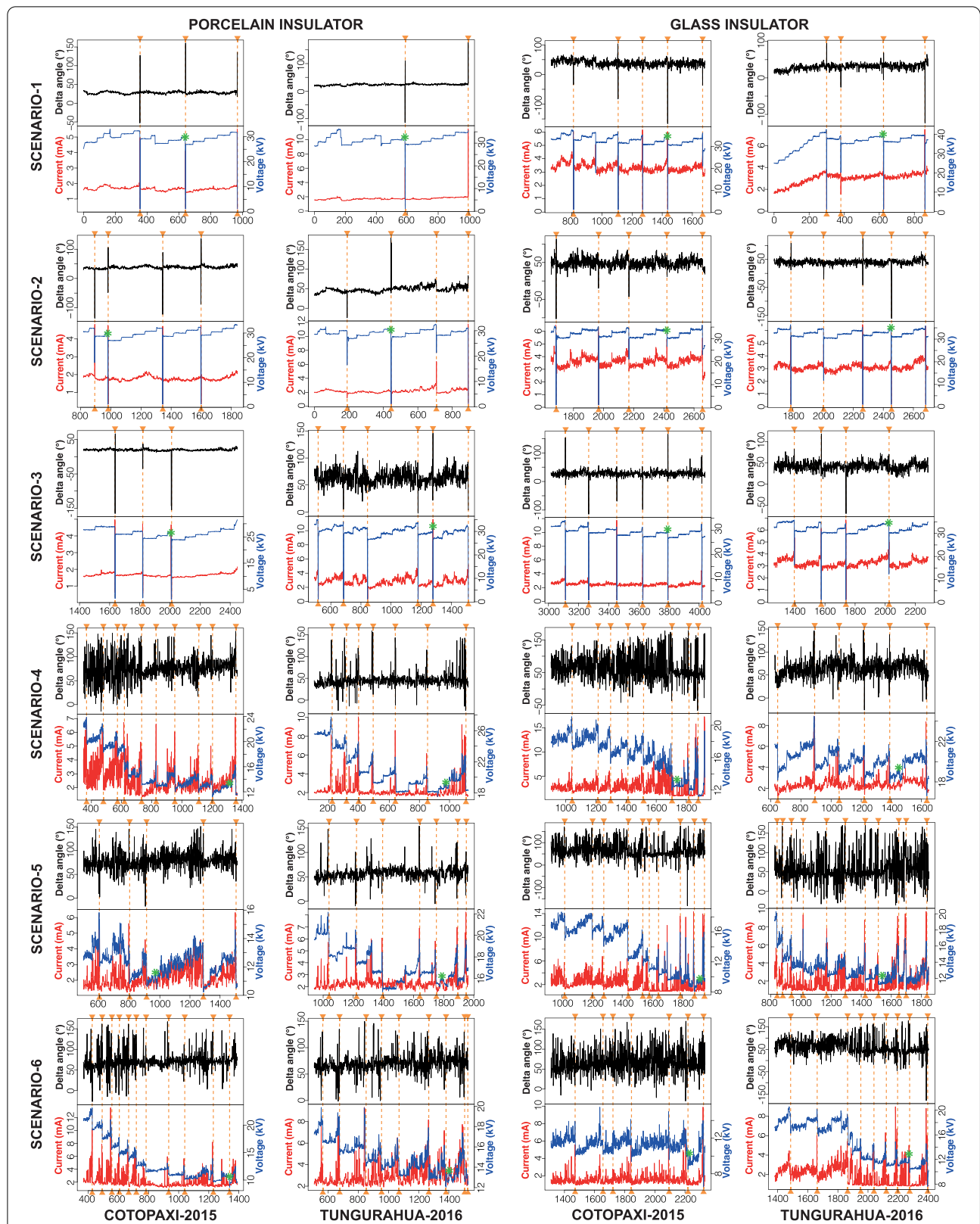


Fig. 8 Dielectric loss factor angle (black), current (red) and voltage (blue) of the porcelain and glass insulators with fresh volcanic ash from Cotopaxi-2015 and Tungurahua-2016 under the six contamination scenarios. Dashed orange lines highlight flashover occurrence and green asterisks depict the FOVmin

failure processes occur under contamination scenarios, it is difficult to identify a current indicator or threshold to forecast a flashover by using the dielectric loss factor angle.

Conductivity and degree of contamination on the insulator (ESDD vs. NSDD)

After each test the residual ash on the insulator was collected and diluted in 500 ml of deionized water to measure its conductivity in Siemens per meter (S/m). As shown in Table 3, overall, the conductivity rises directly proportional to the increase in the amount of ash. Specifically, as the ash layer thickness increases on the top of the insulators from scenarios 1 to 3, so does the conductivity. In scenarios 4 to 6, where ash also blankets the bottom of the insulators, the conductivity of the residual ash is accordingly higher. In addition, a slightly higher conductivity is measured on the glass insulators in comparison to the porcelain ones in all six scenarios. Finally, by comparing both ash types per scenario and insulator model, we observe that the ash from Cotopaxi-2015 is, on average, 2.2 and 2.3 times more conductive than that

of Tungurahua-2016 for porcelain and glass insulators, respectively (Table 3).

In a next step, the obtained conductivity was used to calculate ESDD values. Table 4 shows the results of ESDD and NSDD levels in mg/cm² for the ash from Cotopaxi-2015 and Tungurahua-2016 after finishing each testing procedure. Overall, Cotopaxi’s ash has a higher ESDD than Tungurahua, which indicates that it carried a larger amount of leachable elements. Additionally, ESDD and NSDD do not depend on the insulator type (porcelain or glass) (Fig. 9). The ESDD/NSDD ratio over 100 mg.cm⁻² based on the results shown in Table 4 displays linear trends for both ash types (Fig. 9). Cotopaxi’s ash has an ESDD/NSDD ratio of 0.11%, while Tungurahua’s is 0.04%, with the higher value indicating higher leachate content (Fig. 6) and, therefore, a higher potential to conduct electricity.

Discussion

Evaluation of the insulation quality based on the tested electrical parameters

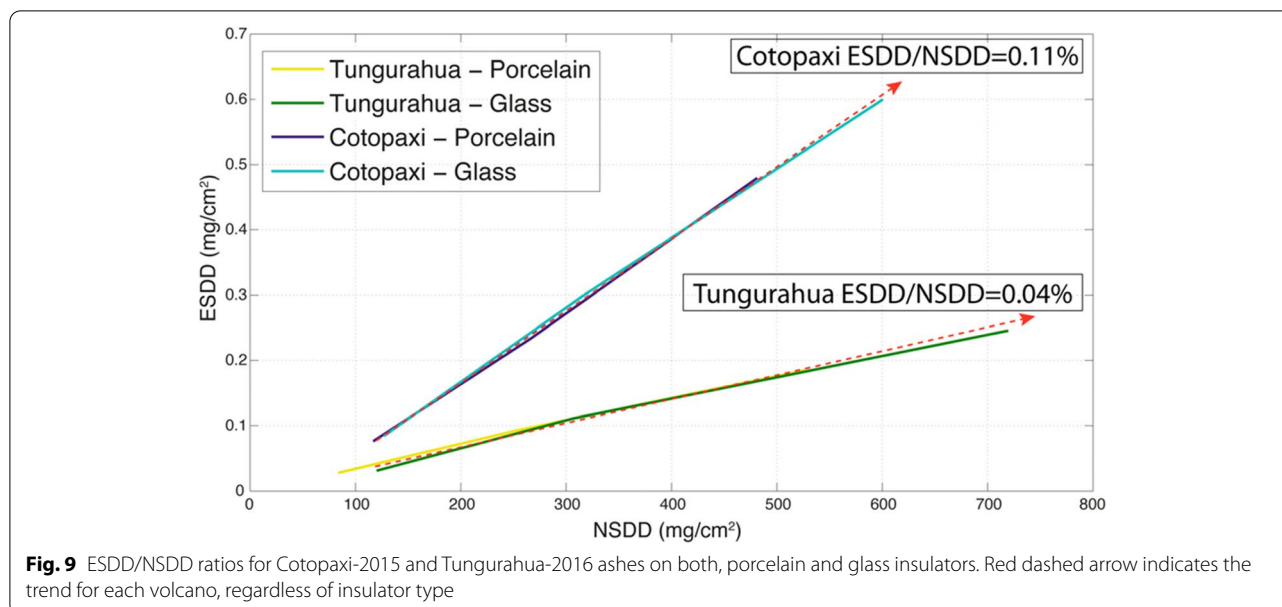
The loss factor angle fluctuated strongly as the conductive leachates dissolved (Fig. 8). These values by

Table 3 Conductivity of the ash collected from the insulators after testing. The ash was diluted in deionized water and the conductivity was corrected for 20 °C

Scenarios	COTOPAXI-2015 conductivity (S/m)		TUNGURAHUA-2016 conductivity (S/m)		Comparison Cotopaxi / Tungurahua	
	Porcelain	Glass	Porcelain	Glass	Porcelain	Glass
1	0.0126	0.0156	0.0047	0.0059	2.7	2.6
2	0.0376	0.0531	0.0154	0.0204	2.4	2.6
3	0.0753	0.1047	0.0299	0.0441	2.5	2.4
4	0.0407	0.0547	0.0230	0.0339	1.8	1.6
5	0.0631	0.0922	0.0349	0.0428	1.8	2.2
6	0.1173	0.1389	0.0524	0.0635	2.2	2.3
Average					2.2	2.3

Table 4 ESDD and NSDD values in mg/cm² of the volcanic ash from Cotopaxi-2015 and Tungurahua-2016 left on the porcelain and glass insulators after each testing procedure

Scenario	COTOPAXI-2015				TUNGURAHUA-2016			
	Porcelain Insulator		Glass Insulator		Porcelain Insulator		Glass Insulator	
	ESDD	NSDD	ESDD	NSDD	ESDD	NSDD	ESDD	NSDD
1	0.0762	116.86	0.0843	126.94	0.0278	83.64	0.0311	120.12
2	0.2341	266.78	0.2978	314.88	0.0932	254.23	0.1114	307.24
3	0.4793	481.28	0.5998	600.51	0.1853	526.92	0.2458	719.51
4	0.1493	101.56	0.1857	110.56	0.0736	149.31	0.1052	207.51
5	0.2760	221.24	0.4055	278.69	0.1415	293.94	0.1840	407.86
6	0.5991	424.67	0.6947	631.79	0.2430	536.26	0.2954	692.56



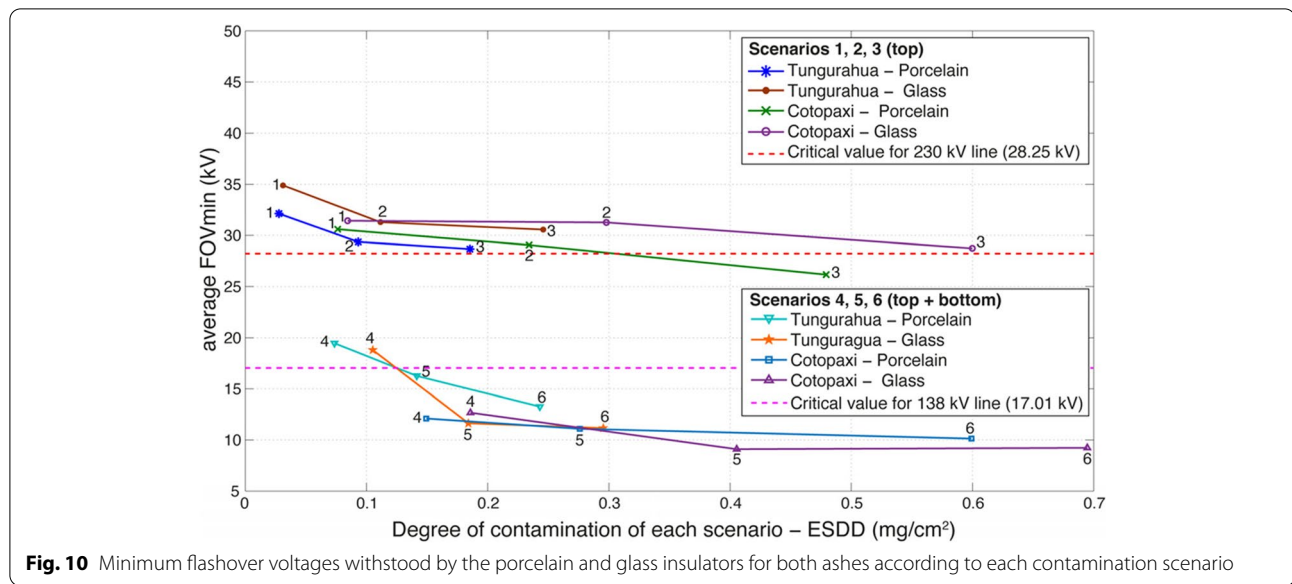
themselves did not provide any anticipatory signal of short-term electrical failure when a constant step-voltage was applied. In scenarios 1 and 2 (contamination on the top), δ reached between 20° and 40° without neither extreme oscillations nor total failure of the insulator under voltages below ~ 20 kV. In contrast, in scenario 6 (top & bottom), δ reached values larger than 100° , but also did not produce total failure under 9 kV (Fig. 8). The increase in the dielectric loss factor angle and its extreme oscillatory nature indicates that the insulator is in a polluted environment and prone to fail because its insulation properties are decreasing. However, under this fluctuating behavior, the critical failure point did not only depend on the dielectric quality, but also on the applied voltage. For instance, in scenario 6, a higher chance of insulator failure only existed when voltages above 9 kV were applied (Fig. 8).

In contrast, to identify the critical point of failure of the insulator, the FOVmin proved to be more suitable than the loss factor method. As shown in Table 2, the minimum voltages that produced a discharge on the insulators (FOVmin) dropped as low as 9 kV under high contamination scenarios. This decrease in voltage that can be withstood from the expected 36 kV under moist conditions to a quarter of this value represents a much higher chance of insulator failure and, thus, probable damage to the entire insulator string and the transmission line. Importantly, while the FOVmin does not serve to anticipate insulator failure in real-time as it cannot be measured at the transmission lines, the critical voltage values presented in Table 2 serve as a

parameter to estimate the possibility of insulator failure during real ash fallout scenarios in Ecuador.

Implications for the Ecuadorian high voltage transmission lines

In this section we analyze whether the contamination scenarios scrutinized in this study are present in Ecuador's transmission lines and determine whether the voltages that the insulators are subjected to are higher than the obtained minimum voltages (FOVmin). To do that, we assumed i) a vertical position for the insulators (no wind influence) and, ii) no parameters from the corona ring. For the transmission line of 230 kV the voltage distribution across the insulator string shows that the highest voltage stress is withstood by the two insulator ends, in particular by the first insulator connected to the conductor (Ashouri et al. 2010). The voltage that the first insulator has to withstand decreases as the number of insulators in the string increases (Ashouri et al. 2010). Under these conditions, we estimated that the most critical voltage that have to be withstood by the first insulator of a 230 kV line with 14 insulators is 28.25 kV or 21.27%. In the same way, we estimated a critical voltage of 17.01 kV (19.64%) that has to be withstood by the first insulator in a line of 138 kV with 10 insulators. Therefore, those ash contamination scenarios that have shown to produce flashover under the critical voltage values of 28.25 kV and 17.01 kV would cause a failure in the insulators string. These two critical voltage values are plotted in Fig. 10, in addition to the average FOVmin as a function of ESDD for the



various contamination scenarios. The data points fall into two clusters based on their scenarios: those in which volcanic ash is deposited only at the top of the insulators (scenario, 1, 2 and 3) produce flashover at voltages between 27 and 35 kV, while those in which volcanic ash blankets the entire insulator (scenarios 4, 5 and 6) do so already from 9 to 20 kV (Fig. 10). In all cases, a higher amount of ash contamination implies a higher percentage of conductive leachates (ESDD), which in the end leads to a lower FOVmin (Fig. 10). Therefore, the average FOVmin decreases as ESDD

increases (Fig. 10), forming a non-linear inverse function (Hussain et al. 2017; Wardman et al. 2014).

For the main Ecuadorian transmission lines, we found that, in the case of the 230 kV line, scenarios 3 (Cotopaxi & Porcelain), 4, 5 and 6 (Cotopaxi-Tungurahua & Porcelain-Glass) would always cause electrical failure (Fig. 10). In addition, scenarios 2 (Cotopaxi & Porcelain), 3 (Cotopaxi & Glass) and 2–3 (Tungurahua & Porcelain) are very close to the critical value and are prone to fail (Fig. 10). For the 138 kV transmission line, in scenarios 4 to 6 electrical failure would occur for Cotopaxi, while

Table 5 Potential transmission lines that would be affected by Cotopaxi and Tungurahua ash and their levels of ash contamination according to the official hazard maps (see Fig. 1), as well as the resulting potential flashover scenarios

COTOPAXI VOLCANO

Hazard Zone	Transmission line	Voltage (kV)	Possible ash thickness (mm)	Contamination scenarios	Potential flashover scenarios
Distal	Santo Domingo – Santa Rosa	230	1 – 10	1–6	3, 4, 5 & 6
	Santo Domingo – Esmeraldas	230	1 – 10	1–6	3, 4, 5 & 6
	Santo Domingo – Quevedo	230	1 – 10	1–6	3, 4, 5 & 6
	Quevedo – San Gregorio	230	1 – 10	1–6	3, 4, 5 & 6
	Quevedo – Pascuales	230	1 – 10	1–6	3, 4, 5 & 6
	Quevedo – Portoviejo	138	1 – 10	1–6	4, 5 & 6
	Quevedo – Chone	138	1 – 10	1–6	4, 5 & 6
	Santo Domingo – Esmeraldas	138	1 – 10	1–6	4, 5 & 6
Proximal	Totoras – Santa Rosa	230	> 100	1–6	3, 4, 5 & 6
	Vicentina – Mulaló – Pucará	138	> 100	1–6	4, 5 & 6

TUNGURAHUA VOLCANO

Distal	Totoras – Ambato	138	3 – 5	1–6	5 & 6
Intermediate	Totoras – Baños – Puyo	138	5 – 8	1–6	5 & 6
Proximal	Totoras – Riobamba – Molino	230	> 8	1–6	3, 4, 5 & 6

for Tungurahua it would only occur in scenarios 5 and 6 (Fig. 10). For contamination scenarios 1 to 3 (contamination at the top of the insulator), no electrical failure is expected (Fig. 10). Due to the complex processes occurring at the insulators during ash pollution in a moist environment, we propose a simple impact evaluation for the most exposed transmission lines (Table 5). The evaluation is based on the eruptive scenarios presented in Fig. 1a and the results from Fig. 10. We took into account the transmission lines which cross the ash fallout hazard zone of Cotopaxi and Tungurahua volcanoes. The impact evaluation considers the voltage distribution at the insulator strings and ash-thickness data from official hazard maps published by the IG-EPN. Here we assume a similar ash leachate content in future ash fallout than that of 2015 for Cotopaxi and 2016 for Tungurahua.

Analysis of the case studies, implications for monitoring future eruptions and possible preventive strategies

Overall, our study finds that the more insulator surface area is covered in ash and the thicker the ash layer, the higher are the chances of insulator failure. Moreover, our findings indicate a visible difference in the negative impact on the dielectric properties of insulators between the fresh volcanic ash of Cotopaxi-2015 and Tungurahua-2016 eruptions. In the case of Cotopaxi-2015, the FOV_{min} occurs at lower values than for Tungurahua-2016 because of its higher leachate content, which leads to a higher conductivity and higher ESDD/NSDD ratio and a lower Cl/SO₄ ratio (Figs. 6 & 7, Tables 2, 3 & 4). The higher leachate content and the lower Cl/SO₄ ratio in Cotopaxi-2015 ash could have resulted from: i) the hydromagmatic nature of the eruption, i.e. interaction of the magma body with a hydrothermal system (Calahorra-Di Patre et al. 2019; Gaunt et al. 2016), and/or ii) significant gas-particle interaction during the eruption, in which a total of 470 kt of SO₂ were emitted from 14 August to 30 November 2015 with an average of 4352 t/day (Hidalgo et al. 2018). In contrast, during the Tungurahua-2016 eruption a total of 12 kt of SO₂ were expelled in 14 days, with an average of 840 t/day (IGEPN 2017). Moreover, the higher fine ash content in Cotopaxi-2015 ash (44%) than in that of Tungurahua-2016 (30%) further increases the amount of leachable elements that can be incorporated (Armienta et al. 2002; Rubin et al. 1994).

Our results highlight the importance of monitoring ash fallout in near real-time. Some parameters such as: componentry, grain size and ash thickness, conductivity, and SO₂ masses and/or daily flux, and, if possible, the amount of leachates are crucial to predict the impact of the volcanic ash on the dielectric characteristics of suspension insulators at electric transmission lines. Rapid testing must be carried out to determine some of these

parameters to better understand the nature and size of a given eruption and its potential impact on electrical infrastructure. In particular, the close relationship between conductivity and ESDD (i.e. leachate content) shows a potential to become a rapid test to find out if fresh volcanic ash has sufficient leachates to produce flashover on the electric insulators. Moreover, the height of eruptive plumes (i.e. erupted ash volume) can serve as input parameter for numerical simulations to rapidly estimate possible ash deposition areas and thicknesses, and to identify possible affected transmission lines and contamination scenarios and, thus, anticipate flashover occurrence. Other parameters related to the weather conditions that should be monitored are wind direction and speed during and after the eruption, as well as moisture levels. Finally, a proper bi-directional communication between the institutions in charge of power supply and monitoring volcanoes based on a well-organized early warning system could prevent the negative impact of future eruptions on the power supply.

Currently, CELEC-EP, the governmental institution in charge of the power supply in Ecuador, considers several pollutants, such as sea-spray and industrial smoke, when deciding on high voltage transmission line layout. However, volcanic ash contamination is not yet taken into account. Based on our results, some mitigation strategies can be explored for preventing flashover occurrence due to volcanic ash pollution on the most exposed high voltage transmission lines. For instance, for transmission lines which traverse volcanic hazard zones, hydrophobic insulators could be installed, and/or a higher number of insulators could be added to the existing strings. Based on our results, ideally no insulator should have to withstand more than 9 kV on the string, if flashover is to be avoided in any volcanic ash contamination scenario. Future work should focus on determining the number of insulators needed to reduce the voltage from 28.25 kV or 17.01 kV to 9 kV for both, the 230 and 138 kV transmission lines and the associated costs and benefits. Finally, in the short-term, during an eruption, electrical failure could be prevented by cleaning insulators regularly with pressurized water.

Limitations

One of the main limitations of this study is related to ash sampling, which was done at only one location for each of the two scrutinized eruptions. For Cotopaxi-2015 the ash was sampled 3 km away from the high voltage transmission line Santa Rosa – Mulaló, while for Tungurahua-2016 it was sampled at 9 km to the Baños – Totoras transmission line (Fig. 1a). No further samples were taken, since the aim of this study was solely to compare if ashes from two different eruptions (i.e. hydromagmatic

and magmatic) had different impact levels on the dielectric characteristics of suspension insulators. Therefore, future analysis focused on a single eruption should perform detailed sampling along possibly exposed transmission lines to assess spatial changes in relevant ash properties such as fine-ash content, conductivity and leachate content and study the effect these spatial variations have on the insulation properties.

A second important limitation regards the characteristics of the insulators used in the laboratory environment. The insulators used were clean and in good conditions, which does not necessarily have to be the case for the insulators already installed and working in the transmission lines. For instance, the age and material deterioration of the insulators, as well as previous surface contamination by pollutants such as urban dust, sea-spray and industrial smoke, could change the effects of volcanic ash on the dielectric properties of the insulators. Thus, the impact of real ash fallout on the transmission lines could differ from the results presented here.

Lastly, our study was conducted under normal power frequency voltage conditions, which means that for a 230 kV transmission line, we expected the insulator string to be subjected to that exact voltage. However, in functioning transmission lines, external energy discharges, such as lightning, can cause for 1000 s of kV to pass through the transmission line for a few milliseconds. Under no-contamination and good insulator quality, such short-lived high discharges are withstood. Based on our results, however, volcanic ash contamination significantly lowers the dielectric characteristics of insulators, suggesting that insulators under contaminated conditions might no longer support discharges of this type. This hypothesis should be further explored in future work using lightning impulse overvoltages.

Conclusion

- The FOV_{min} allows to determine the critical power frequency voltage levels at which a flashover occurs at an insulator under volcanic ash contamination and moist conditions, allowing to assess insulator failure probability for exposed transmission lines.
- The dielectric loss factor angle does not provide any precursory signal to anticipate flashover occurrence, but its strongly oscillating behavior can indicate if an insulator is under a polluted environment.
- The higher the surface area of the insulator covered in ash and the thicker the ash layer is, the worse is the insulation quality and the lower is the critical voltage needed for a flashover.
- The leachate content is higher in Cotopaxi-2015 hydromagmatic ash than in the magmatic ash of Tungurahua-2016. Consequently, the conductivity of the former is more than doubles the latter, and its negative impact on the dielectric quality of the ANSI52-3 suspension insulators is higher.
- In the contamination scenarios in which volcanic ash covers the top insulator surface only, no electric failure is expected in the 138 kV transmission line. On the other hand, in the 230 kV line, those scenarios with 3 and 6 mm of ash blanketing the top of the insulator have a low chance of flashover under moist conditions. This is especially true for porcelain insulators, regardless of ash type, and for Cotopaxi-2015 ash on the glass insulator.
- In those ash contamination scenarios in which the top and bottom of the insulators are blanketed with ash, there is a higher chance that a flashover is produced in both, the 230 kV and 138 kV transmission lines. Only in the case of a 138 kV transmission line of which the insulators (porcelain or glass) are covered on both sides with a 1 mm thick layer of Tungurahua-2016 ash, flashover occurrence is less likely.
- In addition to volcanic ash contamination and moisture, we found that voltage plays a very important role during failure occurrence. If the insulator is subjected to ash contamination under moist conditions with low voltage values, it generally does not fail. On the other hand, if the voltage is continuously increased it is very likely that the insulator will fail under the same polluted conditions.
- Our results show that the minimum critical voltage leading to insulator flashover under highly contaminated conditions lies at 9 kV. Consequently, a possible preventive measure could be to increase the number of insulators in transmission line strings, so that no insulator has to withstand a higher voltage than that.
- Ecuador is a country with various active volcanoes, of which most can produce volcanic ash plumes that can affect electrical transmission lines in wide areas. Therefore, near real-time monitoring of volcanic eruptions, including ash thickness, grain size distribution and ash conductivity, in addition to a well-developed bi-directional communication system between the institutions in charge of the power supply and monitoring volcanoes could prevent blackouts during eruptions.
- In case of sudden eruptive events with large eruptive plumes, numerical simulations of volcanic ash fallout could be performed to provide information about the likely ash fall thickness on the transmission lines. This information could be used to plan insulator string cleaning in a timely manner before a flashover can occur.

Abbreviations

NSDD: Non-soluble deposit density; ESDD: Equivalent soluble deposit density; Mg^{2+} : Magnesium; Na^+ : Sodium; Ca^{2+} : Calcium; K^+ : Potassium; Cl^- : Chlorine; F^- : Fluorine; S^{2-} : Sulfur; SO_4^{2-} : sulphates; kV: Kilovolts; IG-EPN: Instituto Geofísico de Escuela Politécnica Nacional; AD: Anno Domini; BP: Before the Present; GSD: Grain Size Distribution; F1: Coarse ash (< 1 mm); F2: Fine ash (< 63 μm); Md: Median of GSD; D16: Percentile at 16 in GSD; D84: Percentile at 84 in GSD; EPN: Escuela Politécnica Nacional; FOVmin: Minimum Insulator Flashover Voltage; atm: Atmospheric pressure; KVM: Kilovoltmeter; C1 & C2: Capacitor; ADC: Analogue Digital Converter; IRs: Real component of an electric current; $I/\omega.Cs$: Reactive component of an electric current; AC: Alternating current; Ix: Current passing through the insulator; Is: Reference current; A: Ampere; mA: Milliampere; Rx: Insulator resistor; Cx: Insulator capacitor; Cs: Reference capacitor; R1 & R2: Power resistors; DAQ NI USB-6008: Data acquisition card; RMS: Root mean square; Std: Standard deviation; RFO: Rapid Flashover Procedure; S: Siemens; m: Meter; t: Tons; kt: Kilotons; SO_2 : Sulfur dioxide; CELEC-EP: Governmental institution in charge of power supply in Ecuador.

Acknowledgements

The authors thank the Departamento de Energía Eléctrica and the Instituto Geofísico de la Escuela Politécnica Nacional (IG-EPN) for the logistical support during this research. The CICAM for providing chemical analysis of the leachates. A special acknowledgment goes to Victor Roberto Zumba vigía from Choglontus who kindly helped to collect the Tungurahua's ash used in this investigation. This research was conducted in the context of IG-EPN's project "Generación de Capacidades para la Emisión de Alertas Tempranas" funded by Secretaría Nacional de Planificación y Desarrollo (SENPLADES) and the Escuela Politécnica Nacional.

Authors' contributions

JR and AL performed the testing procedure on the suspension insulators. FJV and SH lead the leachate analysis. JR, AL, FJV and BB collected the fresh volcanic ash samples that were analyzed. JR, AL, FV, and FQ conceived and designed the experimental procedure. FJV, AVM, JR, AL, SH and BB wrote the manuscript. All the authors read and approved the final version of the article.

Funding

Not applicable.

Availability of data and materials

There is no additional data.

Declarations

Competing interests

The authors declare that they have no competing interests.

Author details

¹Departamento de Energía Eléctrica. Escuela Politécnica Nacional, Quito, Ecuador. ²Instituto Geofísico. Escuela Politécnica Nacional, Quito, Ecuador. ³Departamento de Control en Tiempo Real, Empresa Eléctrica Quito, Quito, Ecuador. ⁴School of Earth Sciences, University of Bristol, Bristol BS8 1RJ, UK.

Received: 14 July 2021 Accepted: 29 May 2022

Published online: 23 June 2022

References

- Andújar J, Martel C, Pichavant M, Samaniego P, Scaillet B, Molina I (2017) Structure of the Plumbing System at Tungurahua Volcano, Ecuador: Insights from Phase Equilibrium Experiments on July–August 2006 Eruption Products. *J Petrol* 58(7):1249–1278
- Arellano SR, Hall M, Samaniego P, Le Pennec J-L, Ruiz A, Molina I et al (2008) Degassing patterns of Tungurahua volcano (Ecuador) during the 1999–2006 eruptive period, inferred from remote spectroscopic measurements of SO_2 emissions. *J Volcanol Geoth Res* 176(1):151–162
- Barberi F, Coltelli M, Frullani A, Rosi M, Almeida E (1995) Chronology and dispersal characteristics of recently (last 5000 years) erupted tephra of Cotopaxi (Ecuador): implications for long-term eruptive forecasting. *J Volcanol Geoth Res* 69(3):217–239
- Battaglia J, Hidalgo S, Bernard B, Steele A, Arellano S, Acuña K (2019) Autopsy of an eruptive phase of Tungurahua volcano (Ecuador) through coupling of seismo-acoustic and SO_2 recordings with ash characteristics. *Earth Planet Sci Lett* 511:223–232
- Bernard B, Battaglia J, Proaño A, Hidalgo S, Váscquez F, Hernandez S et al (2016) Relationship between volcanic ash fallouts and seismic tremor: quantitative assessment of the 2015 eruptive period at Cotopaxi volcano, Ecuador. *Bull Volcanol* 78(11):80
- Biasi S, Bonadonna C (2013) A fast GIS-based risk assessment for tephra fallout: the example of Cotopaxi volcano, Ecuador. Part I: probabilistic hazard assessment. *Nat Hazards* 65(1):477–495
- Cáceres BE (2016) Dramatical reduction of Cotopaxi Glaciers during the last volcano awakening 2015–2016. *AGUFM 2016:C41C-0677*
- Calahorrano-Di Patre A, Williams-Jones G, Battaglia M, Mothes P, Gaunt E, Zurek J et al (2019) Hydrothermal fluid migration due to interaction with shallow magma: Insights from gravity changes before and after the 2015 eruption of Cotopaxi volcano, Ecuador. *J Volcanol Geoth Res* 387:106667
- Delmelle P, Gerin P, Oskarsson N (2000) Surface and bulk studies of leached and unleached volcanic ashes. *EOS Trans AGU* 81:F1311
- Delmelle P, Lambert M, Dufrière Y, Gerin P, Óskarsson N (2007) Gas/aerosol–ash interaction in volcanic plumes: New insights from surface analyses of fine ash particles. *Earth Planet Sci Lett* 259(1–2):159–170
- Eychenne J, Le Pennec J-L (2012) Sigmoidal particle density distribution in a subplinian scoria fall deposit. *Bull Volcanol* 74(10):2243–2249
- Forte P, Domínguez L, Bonadonna C, Gregg CE, Bran D, Bird D et al (2018) Ash resuspension related to the 2011–2012 Cordón Caulle eruption, Chile, in a rural community of Patagonia, Argentina. *J Volcanol Geoth Res* 350:18–32
- Hall ML, Robin C, Beate B, Mothes P, Monzier M (1999) Tungurahua Volcano, Ecuador: structure, eruptive history and hazards. *J Volcanol Geoth Res* 91(1):1–21
- Hall ML, Steele AL, Bernard B, Mothes PA, Vallejo SX, Douillet GA et al (2015) Sequential plug formation, disintegration by Vulcanian explosions, and the generation of granular Pyroclastic Density Currents at Tungurahua volcano (2013–2014), Ecuador. *J Volcanol Geoth Res* 306:90–103
- Hidalgo S, Battaglia J, Arellano S, Steele A, Bernard B, Bourquin J et al (2015) SO_2 degassing at Tungurahua volcano (Ecuador) between 2007 and 2013: Transition from continuous to episodic activity. *J Volcanol Geoth Res* 298:1–14
- Le Pennec J-L, Jaya D, Samaniego P, Ramón P, Moreno Yáñez S, Egred J et al (2008) The AD 1300–1700 eruptive periods at Tungurahua volcano, Ecuador, revealed by historical narratives, stratigraphy and radiocarbon dating. *J Volcanol Geoth Res* 176(1):70–81
- Le Pennec J-L, Ruiz GA, Ramón P, Palacios E, Mothes P, Yepes H (2012) Impact of tephra falls on Andean communities: The influences of eruption size and weather conditions during the 1999–2001 activity of Tungurahua volcano, Ecuador. *J Volcanol Geoth Res* 217–218:91–103
- Mothes P, Hall ML, Andrade D, Yepes H, Pierson TC, Gorki Ruiz A et al (2004) Character, stratigraphy and magnitude of historical lahars of Cotopaxi volcano (Ecuador). *Acta Vulcanol* 16(1/2):1000–1023
- Mothes P, Yepes HA, Hall ML, Ramón PA, Steele AL, Ruiz MC (2015) The scientific–community interface over the fifteen-year eruptive episode of Tungurahua Volcano, Ecuador. *J Appl Volcanol* 4(1):9
- Parra R, Bernard B, Narváez D, Le Pennec J-L, Hasselle N, Folch A (2016) Eruption Source Parameters for forecasting ash dispersion and deposition from vulcanian eruptions at Tungurahua volcano: Insights from field data from the July 2013 eruption. *J Volcanol Geoth Res* 309:1–13
- Pistolesi M, Rosi M, Cioni R, Cashman KV, Rossotti A, Aguilera E (2011) Physical volcanology of the post-twelfth-century activity at Cotopaxi volcano, Ecuador: Behavior of an andesitic central volcano. *Geol Soc Am Bull* 123(5–6):1193–1215
- Ramon P, Vallejo Vargas S, Mothes PA, Andrade SD, Vasquez FJ, Yepes H et al (2021) Instituto Geofísico – Escuela Politécnica Nacional, the Ecuadorian Seismology and Volcanology Service. *Volcanica* 4(1):93–112
- Samaniego P, Le Pennec J-L, Robin C, Hidalgo S (2011) Petrological analysis of the pre-eruptive magmatic process prior to the 2006 explosive eruptions at Tungurahua volcano (Ecuador). *J Volcanol Geoth Res* 199(1–2):69–84

- Taylor PS, Stoiber RE. Soluble material on ash from active Central American volcanoes. *Geological Society of America Bulletin*. Geological Society of America; 1973;84(3):1031–42.
- Wadhwa CL. *High Voltage Engineering*. 2nd ed. New Delhi: New Age International Ltd; 2007.
- Wardman JB, Wilson T, Hardie S, Bodger P. Influence of volcanic ash contamination on the flashover voltage of HVAC outdoor suspension insulators. *IEEE Transactions on Dielectrics and Electrical Insulation*. IEEE; 2014;21(3):1189–97.
- Wardman JB, Wilson TM, Bodger PS, Cole JW, Johnston DM. Investigating the electrical conductivity of volcanic ash and its effect on HV power systems. *Physics and Chemistry of the Earth, Parts A/B/C*. Elsevier; 2012;45:128–45.
- Wilson G, Wilson TM, Deligne NI, Cole JW. Volcanic hazard impacts to critical infrastructure: A review. *Journal of Volcanology and Geothermal Research*. Elsevier; 2014;286:148–82.
- Witham CS, Oppenheimer C, Horwell CJ. Volcanic ash-leachates: a review and recommendations for sampling methods. *Journal of volcanology and Geothermal Research*. Elsevier; 2005;141(3–4):299–326.
- Wolf T. Memoria sobre el Cotopaxi y su última erupcion, acaecida el 26 de junio de 1877, por Teodoro Wolf: Con una lámina y una carta topográfica. Imp. del comercio; 1878.

Publisher's Note

Springer Nature remains neutral with regard to jurisdictional claims in published maps and institutional affiliations.

Ready to submit your research? Choose BMC and benefit from:

- fast, convenient online submission
- thorough peer review by experienced researchers in your field
- rapid publication on acceptance
- support for research data, including large and complex data types
- gold Open Access which fosters wider collaboration and increased citations
- maximum visibility for your research: over 100M website views per year

At BMC, research is always in progress.

Learn more biomedcentral.com/submissions

